electronics, which we refer to as "nanoelectronics."

REFERENCES AND NOTES

1. For reviews, see: C. F. Quate, in *Highlights of the 80's and Prospects for the 90's in Condensed Matter Physics*, L. Esaki, Ed. (Plenum, New York, 1991); G. M. Shedd and P. E. Russel, *Nanotechnology* **1**, 67 (1990).
2. G. Binnig, H. Rohrer, Ch. Gerber, E. Weibel, *Phys. Rev. Lett.* **49**, 59 (1982).
3. R. Gomer, *IBM J. Res. Dev.* **30**, 428 (1986).
4. R. S. Becker, J. A. Golovchenko, B. S. Swartzentrouber, *Nature* **325**, 419 (1987).
5. J. S. Foster, J. E. Frommer, P. C. Arnett, *ibid.* **331**, 324 (1988).
6. R. Emch, J. Nogami, M. M. Dovek, C. A. Lang, C. F. Quate, *J. Microsc.* **152**, 129 (1988).
7. Y. Z. Li, L. Vazquez, R. Piner, R. P. Andres, R. Reifenberger, *Appl. Phys. Lett.* **54**, 1424 (1989).
8. I.-W. Lyo and Ph. Avouris, *J. Chem. Phys.* **93**, 4479 (1990).
9. H. M. Mamin, P. H. Guether, D. Rugar, *Phys. Rev. Lett.* **65**, 2418 (1990).
10. L. J. Whitman, J. A. Stroscio, R. A. Dragoset, R. J. Celotta, *Science* **251**, 1206 (1991).
11. Ph. Avouris and R. Wolkow, *Phys. Rev. B* **39**, 509 (1989).
12. T. T. Tsong, *Atom-Probe Field Ion Microscopy* (Cambridge Univ. Press, Cambridge, 1990), and references therein.
13. G. Binnig and H. Rohrer, *Surf Sci.* **126**, 236 (1983).
14. J. K. Gimzewski and R. Möller, *Phys. Rev. B* **36**, 1284 (1987).
15. N. D. Lang, *ibid.* **37**, 10395 (1988).
16. S. Ciraci and E. Tekman, *ibid.* **40**, 11969 (1989).
17. P. F. Marella and R. F. Pease, *Appl. Phys. Lett.* **55**, 2366 (1989).

18. We thank N. Lang for helpful discussions and J. E. Demuth and R. Walkup for a careful reading of the manuscript.

7 May 1991; accepted 13 June 1991

Rapid Eruption of the Siberian Traps Flood Basalts at the Permo-Triassic Boundary

PAUL R. RENNE AND ASISH R. BASU

The Siberian Traps represent one of the most voluminous flood basalt provinces on Earth. Laser-heating $^{40}Ar/^{39}Ar$ data indicate that the bulk of these basalts was erupted over an extremely short time interval (900,000 ± 800,000 years) beginning at about 248 million years ago at mean eruption rates of greater than 1.3 cubic kilometers per year. Such rates are consistent with a mantle plume origin. Magmatism was not associated with significant lithospheric rifting; thus, mantle decompression resulting from rifting was probably not the primary cause of widespread melting. Inception of Siberian Traps volcanism coincided (within uncertainty) with a profound faunal mass extinction at the Permo-Triassic boundary 249 ± 4 million years ago; these data thus leave open the question of a genetic relation between the two events.

AT LEAST 11 DISTINCT EPISODES OF voluminous volcanism have produced flood basalt provinces covering more than 100,000 km^2 in the last 250 million years (*1–3*). The eruption of major flood basalt provinces is generally attributed to the thermal anomaly generated by a subcontinental mantle plume or hot spot (*2, 4–6*). The plume model predicts that initial rapid and voluminous flood basalt eruptions are followed by dimunition of eruption rate and in some cases the production of a hotspot track as a lithospheric plate moves over the mantle plume (*2, 4*).

The paroxysmic effusion of magma and volcanic gases that characterizes initial flood basalt activity may sufficiently disrupt Earth's atmospheric and hydrospheric cycles that biotic crises result (*1, 7, 8*): A celebrated possible example is the eruption of the Deccan Traps, which has been inferred as a mechanism for the Cretaceous-Tertiary faunal mass extinction event (*7*). Comprising roughly 1.5 × 10^6 km^3 of lava, most of the Deccan Traps may have been erupted during a period of less than 1 million years at about 66 Ma (million years ago), coincident within uncertainties with the Cretaceous-Tertiary boundary (*3, 9*). Compelling evidence has also been raised for a meteorite impact at the Cretaceous-Tertiary boundary; this is thought by many to represent a more likely cause for this extinction (*10*).

Some investigators have proposed a relation between major flood basalt events and bolide impacts: Both have been inferred to show a periodicity of 26 to 32 million years that may be in phase and may correlate temporally with periodic faunal mass extinction events (*1*). Uncertainties in the age and duration of many flood basalt provinces, however, inhibit precise temporal correlation between flood basalt episodes, mass extinctions, and bolide impacts.

Arguably the largest Phanerozoic flood basalt province is the Siberian Traps (ST; Fig. 1), which now cover ~3.4 × 10^5 km^2 and which may have had an original volume of >1.5 × 10^6 km^3 (*11–13*). In this report, we present high-precision $^{40}Ar/^{39}Ar$ geochronologic data showing that most of the ST were erupted over a very short time interval (~1 million year) coinciding, within uncertainties, with the Permo-Triassic extinction event that marked the end of the Paleozoic Era.

The ST occur on the northwestern margin of the Siberian Platform where they overlie Carboniferous to Upper Permian lagoonal and terrestrial sedimentary rocks. The flood basalts have a composite thickness greater than 3700 m and include basaltic flows and volumetrically minor basaltic tuffs; significant local variations in thickness apparently reflect basin geometry and the distribution of vents (*12, 14*).

The ST comprise a stratigraphic succession of petrologically distinct suites of flows that are laterally continuous over tens of kilometers. In the Noril'sk region, where at least 45 flows produce the greatest thickness of flows, the ST have been divided into 11 suites (Fig. 2) (*11–13*). Stratigraphic sections elsewhere in the ST can be correlated readily with the Noril'sk section (*13, 15*).

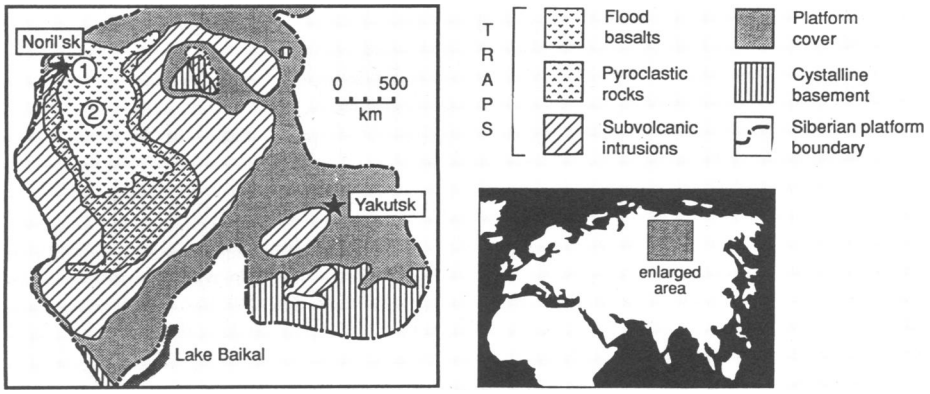

Fig. 1. Geologic sketch map of part of the Siberian platform showing the distribution of the Siberian Traps [after (*11*)]. Circled numbers indicate locations of the Noril'sk (1) and Putorana (2) sections.

P. R. Renne, Institute of Human Origins, Geochronology Center, 2453 Ridge Road, Berkeley, CA 94709.
A. R. Basu, Department of Geological Sciences, University of Rochester, Rochester, NY 14627.

The lack of significant sedimentary rocks or paleosols in the section implies that little time elapsed between eruptions.

Whole-rock ^{40}K-^{40}Ar dates of ST lavas have led to disparate conclusions about the age and duration of volcanism. Zolotukhin and Al'Mukhamedov (*11*) estimated that eruption was concentrated between 235 and 220 Ma but lasted from 240 to 200 Ma. Other workers (*16, 17*) reported dates from the Russian literature that clustered between 240 and 250 Ma.

A Permo-Triassic age for the ST has been dismissed by Baksi and Farrar (*3*) on the basis of conventional whole-rock incremental-heating $^{40}Ar/^{39}Ar$ data from two lava flows stated to occur near the bottom (238.4 ± 1.4 Ma) and near the top (229.9 ± 2.3 Ma) of the volcanic succession (1σ errors). These samples come from south of our Putorana section (Fig. 1), far from the thickest accumulations of ST lavas, and may not be representative of the main pulse of ST volcansim, although their Nd and Sr isotopic compositions are consistent with those of ST lavas from the northern part of the province (*13*). Baksi and Farrar (*3*) interpreted these data to (i) preclude a relation between the ST and the Permo-Triassic mass extinction event and (ii) to indicate a relatively long (5 to 10 million years) duration for ST volcanism in contrast with the shorter durations (<2 million years) of flood basalt provinces for which the best geochronologic data are available (for example, the Deccan Traps of India and the Columbia River basalts of the western United States). Such a duration for the main pulse of ST volcanism would imply that mean eruption rates were less than 0.3 km^3 per year, significantly less than mean rates for other flood basalt provinces (*2*) and possibly inconsistent with the notion of a mantle plume origin of the ST.

We dated samples of selected ST flows spanning most of the succession in order to clarify the duration of volcanism and its possible coincidence with the Permo-Triassic boundary. The dated samples were among those analyzed in a separate petrologic-isotopic study (*13*), and our sample numbers correspond to those used in that study. Whole-rock samples (*18*) were prepared from samples 46 and 2. Whole-rock samples were holocrystalline and coarse-grained; thus, the effects of ^{39}Ar recoil loss and redistribution (*19*) were minimized, and the possibility of Ar or K mobility arising from alteration of glass was eliminated. Petrographically visible alteration of the samples is confined to minor chloritization of olivine. Optically clear, unaltered plagioclase was separated from samples 46 and 42. Samples were irradiated for 28 hours in the Omega West nuclear reactor at Los Alamos National Laboratory to generate ^{39}Ar by the $^{39}K(n, p)^{39}Ar$ reaction. Fish Canyon sanidine, with a reference age of 27.84 Ma, was used as a fast neutron fluence monitor (*20*). Analytical procedures are outlined in (*21*).

Sample 46 is an aphyric subalkaline basalt flow from the basal (Ivakinsky) suite. This lava contains chiefly plagioclase and titanaugite and has a coarse (average grain size ~0.5 mm) subophitic texture. Separate whole-rock analyses yielded well-defined apparent age plateaus (Table 1) (*22*) for more than 80 to 90% of the ^{39}Ar released (Fig. 3). Anomalously low apparent ages in the low-temperature release fractions indicate that minor amounts of radiogenic $Ar(^{40}Ar^*)$ were lost. The two whole-rock plateau dates (248.5 ± 0.8 and 248.3 ± 0.4 Ma) agree with one another and with plateau dates (248.1 ± 0.8 and 248.7 ± 0.7 Ma) from two bulk samples of plagioclase separated from this lava. Because all four plateau dates for this flow coincide within uncertainty, a mean of 248.4 ± 0.3 Ma was calculated from 25 plateau steps from all four step-heating runs. The high precision obtained is not simply an artifact of the large number of analyses with individually low uncertainties; the arithmetic mean of the four plateau dates from this sample is also 248.4 ± 0.3 Ma (2 SE).

Plagioclase was analyzed from a tholeiitic picrite basalt flow (sample 42) in the Gudchikhinsky suite higher in the Noril'sk section. The lava is coarse grained (average grain size ~1.0 mm) and has a subophitic texture and cumulate olivine. Plateaus were obtained in two step-heating runs, although both runs show some evidence for partial $^{40}Ar^*$ loss. The two plateau dates (247.4 ± 1.6 and 247.6 ± 1.6 Ma) are statistically indistinguishable; therefore, a mean plateau date of 247.5 ± 1.1 Ma was calculated from all ten plateau steps from the two runs.

Whole-rock samples were analyzed from an aphyric basalt flow (sample 2) from the uppermost Nerakarsky suite of the Putorana section, which is correlated with the Kharaelakhsky suite at Noril'sk. The lava is medium grained (average grain size is ~0.3 mm), composed chiefly of plagioclase and clinopyroxene, and has a poikilophitic texture. Samples yielded discordant apparent age spectra reflecting the effects of both minor $^{40}Ar^*$ loss and ^{39}Ar recoil redistribution (*19*). The first analysis failed to define an apparent age plateau, but more detailed incremental heating in a second run delineated a plateau comprising the last eight steps, which yield a plateau date of 247.7 ± 0.7 Ma. Deleting an anomalous step (representing less than 2.1% of the ^{39}Ar in the plateau steps) at 254.7 ± 4.6 Ma yields a plateau date of 247.5 ± 0.7, which we prefer as representing the crystallization age of this sample.

Data acquired by step-heating analysis of each sample were also cast on $^{36}Ar/^{40}Ar$

Noril'sk	Thickness (m)		Putorana
Samoedsky TH	0-800		
Kumingsky TH	0-210		
Kharaelakhsky TH, ASA	380-600	400	Nerakarsky TH
Mukulaevsky TH	400-650	600	Honnamakitsky TH
Morongovsky TH, SA	300-600	800	Ayansky TH
Nadezhdinsky TH, ASA, TF	200-570		
Tuklonsky TH	0-250		
Khakanchansky TF	10-130		
Gudchikhinsky TH, PC	0-200		
Syverminsky TH, ASA	0-240		
Ivakinsky ASA, TH, TF	0-330		

Fig. 2. Generalized composite stratigraphic sections of the Siberian Traps in the Noril'sk and Putorana regions. Stratigraphic positions of the dated samples are indicated by black dots. Sources are from (*11–13*). Petrologic abbreviations shown in order of abundance for each suite: TH, tholeiitic basalt; ASA, alkaline to subalkaline basalt; TF, tuff; and PC, picrite basalt.

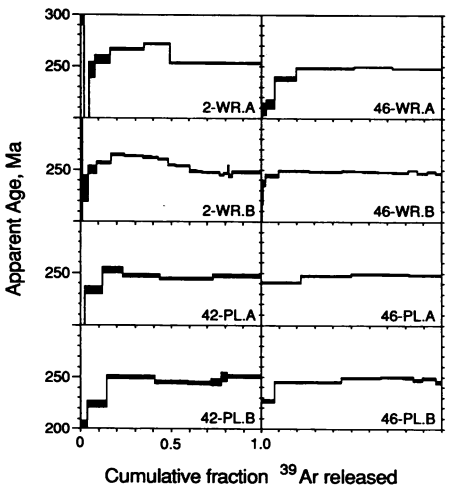

Fig. 3. Apparent age spectra showing apparent age as a function of cumulative fraction ^{39}Ar released for the samples indicated; WR (PL) refer to whole-rock (plagioclase) samples; A and B suffixes refer to the first and second incremental heating experiment performed on each sample. Vertical width of each increment corresponds to 1σ uncertainty in apparent age. Apparent age range for each spectrum plot is 200 to 300 Ma.

versus $^{39}Ar/^{40}Ar$ isotope correlation diagrams, and data from plateau steps were regressed in order to evaluate the isotopic composition of non-radiogenic Ar (hence the validity of the atmospheric correction). Results of this analysis (*23*) are consistent with the plateau dates for each sample, although the uncertainties are higher. The larger errors attending these regressions result from the small ranges in $^{36}Ar/^{40}Ar$ ratios. The small range in ratios corresponds to consistent values of the percent $^{40}Ar^*$ released for each sample (Table 1) after most of the nonradiogenic Ar was degassed in low-temperature steps.

Table 1. Summary of $^{40}Ar/^{39}Ar$ dating results for plateau steps. Errors do not reflect uncertainty in the age of standards. WR (PL) indicates a whole-rock (plagioclase) sample. Laser indicates laser power output, in watts; * indicates sample was fused; (%) $^{40}Ar^*$ is the percentage of ^{40}Ar that is nonatmospheric; and ^{39}Ar is the ion beam signal for ^{39}Ar, in nanoamperes. Full analytical data available from first author upon request.

Laser	(%) $^{40}Ar^*$	^{39}Ar	Date (Ma) ± 2σ
		2-WR.B	
1.8	89.4	0.231	248.9 ± 1.8
1.9	90.1	0.165	248.4 ± 2.1
2.1	88.6	0.531	247.8 ± 1.5
2.3	89.5	0.120	245.4 ± 2.2
2.6	90.5	0.117	246.9 ± 2.3
3.0	91.5	0.046	254.7 ± 4.6
4.0	88.1	0.093	244.3 ± 3.0
8.0*	86.2	0.891	247.9 ± 2.0
		42-PL.A	
1.5	90.5	0.043	252.7 ± 5.3
2.5	93.4	0.074	247.2 ± 3.3
4.0	90.6	0.109	246.3 ± 2.7
8.0*	93.2	0.099	247.2 ± 3.0
		42-PL.B	
1.2	93.6	0.198	249.9 ± 3.2
1.5	96.3	0.136	245.2 ± 3.4
1.9	98.7	0.096	244.9 ± 3.2
3.3	98.6	0.042	245.1 ± 6.4
4.0	99.9	0.024	250.1 ± 8.8
8.0*	99.0	0.143	250.4 ± 3.4
		46-WR.A	
1.5	88.4	0.649	248.3 ± 1.5
2.3	99.0	0.430	249.4 ± 1.3
4.0*	97.7	0.558	247.9 ± 1.3
		46-WR.B	
1.2	90.7	1.415	249.0 ± 1.5
1.3	97.0	0.850	248.3 ± 1.3
1.4	98.3	0.638	248.5 ± 1.3
1.5	98.4	0.565	249.3 ± 1.4
1.6	97.9	0.382	248.9 ± 1.3
1.8	97.8	0.684	248.5 ± 1.3
2.0	97.5	0.659	247.8 ± 1.3
2.2	98.0	0.743	247.6 ± 1.4
2.5	99.7	0.423	249.4 ± 1.4
2.9	98.4	0.449	246.8 ± 1.3
3.4	98.9	0.401	248.1 ± 1.4
3.9*	98.0	0.244	246.9 ± 1.7
		46-PL.A	
1.5	94.0	0.521	247.4 ± 1.4
4.0	90.7	0.621	249.0 ± 1.5
8.0*	99.0	0.338	248.1 ± 1.3
		46-PL.B	
1.2	96.5	0.549	249.1 ± 1.3
1.6	99.1	0.314	249.6 ± 1.4
2.0	99.5	0.139	249.6 ± 1.8
2.5	99.2	0.136	247.1 ± 2.2
3.2	99.7	0.103	248.2 ± 2.1
8.0*	99.7	0.082	248.8 ± 2.5

The significance of discordance represented by the low-temperature portions of each sample's apparent age spectrum is unclear. No K-bearing secondary phases were observed in any of the samples; hence, minor loss of $^{40}Ar^*$ from plagioclase (chief repository of K) due to low grade (≲150°C) reheating is implied. The small portion of $^{40}Ar^*$ lost from each sample is insufficient to undermine credibility of the plateau dates.

On the basis of our data, we are unable to resolve convincingly the ages of the three flows dated; thus the time encompassed by the bulk of ST flood basalt volcanism was very short and nearly within the analytical errors in dating. An estimated minimum of 75% of the total volume (*24*) of the ST represented in the Noril'sk-Putorana region was apparently erupted between 248.3 ± 0.3 and 247.5 ± 0.7 Ma, an interval of 0.9 ± 0.8 (2σ) million years. The implied minimum eruption rate of ~1.3 km^3 per year for all but the stratigraphically youngest lavas is comparable to eruption rates estimated for some of the most prolific flood basalt provinces known, including the Deccan Traps, Karoo Province, and Columbia River Basalts (*1, 2*).

The high eruption rates favor a mantle plume origin (*2, 25*) for this province. The lack of evidence for rifting of the crust before initiation of the ST (*26*) suggests that lithospheric extension was not a necessary condition for mantle plume development in this case; the apparent absence of ST-related rifting has been cited (*25*) as evidence against the case for continental rifting causing widespread melting (*5*) that produces massive flood basalts.

Unlike other major flood basalt provinces (for example, the Deccan Traps, Karoo, Paraná, Columbia River Basalts), the ST are not clearly related to subsequent hot-spot activity, although Morgan (*4*) suggested that they may be related to the Jan Mayen hot spot, currently located north of Iceland. Lightfoot *et al.* (*12*) noted that volcanism in the Noril'sk region progressed northeastward, as would be consistent with an association with the Jan Mayen hot spot, but knowledge of the geology of northern Siberia and the Arctic Ocean is incomplete.

Considering only the analytical precision of our dates for the Siberian Traps is appropriate for assessing the duration of volcanism. However, uncertainty in the age of the neutron fluence monitor must be considered in evaluating the absolute age of volcanism. Allowing a 1% uncertainty in the age of Fish Canyon sanidine (*27*) results in an uncertainty of ±2.4 Ma (2σ) for the age of sample 46, from the basal (Ivakinsky) suite. Thus the inception age and error for the ST is 248.4 ± 2.4 Ma.

Recent estimates for the age of the Permian-Triassic boundary range from 245 to 250 Ma (*28*). Review of these estimates led Rampino and Stothers (*1*) to propose an age of 249 ± 4 Ma. Our data therefore indicate that ST magmatism coincided with the Permian-Triassic faunal mass extinction, within the uncertainties in our dates and in the age of this biostratigraphically defined event. Thus the possibility of a genetic link between ST volcanism and the extinction event must continue to be entertained. The nature and duration of the Permian-Triassic extinctions, and hence their cause, are not well understood (*29*).

Further refinements of the age of the ST can be expected with improved calibration of dating standards. More important for testing precise synchroneity with the Permo-Triassic boundary, however, is refinement of the age of the boundary itself.

REFERENCES AND NOTES

1. M. R. Rampino and R. B. Stothers, *Science* **241**, 663 (1988).
2. M. A. Richards, R. A. Duncan, V. E. Courtillot, *ibid.* **246**, 103 (1989).
3. A. K. Baksi and E. Farrar, *Geology* **19**, 461 (1991).
4. W. J. Morgan, in *The Sea*, C. Emiliani, Ed. (Wiley-Interscience, New York, 1981), vol. 7, pp. 443–475.
5. R. White and D. McKenzie, *J. Geophys. Res.* **94**, 7685 (1989).
6. I. H. Campbell and R. W. Griffiths, *Earth Planet. Sci. Lett.* **99**, 79 (1990).
7. C. O. Officer and C. L. Drake, *Science* **219**, 1383 (1983).
8. W. J. Morgan, *Eos* **67**, 391 (1986).
9. V. Courtillot *et al.*, *Earth Planet. Sci. Lett.* **80**, 361 (1986); V. Courtillot *et al.*, *Nature* **333**, 843 (1988); R. A. Duncan and D. G. Pyle, *ibid.*, p. 841; J.-J. Jaeger, V. Courtillot, P. Tapponier, *Geology* **17**, 316 (1989).
10. L. W. Alvarez *et al.*, *Science* **208**, 1095 (1980); K. J. Hsü, *Nature* **285**, 201 (1980); W. Alvarez and R. A. Muller, *ibid.* **308**, 718 (1984); M. R. Rampino and R. B. Stothers, *Science* **226**, 1427 (1984).
11. V. V. Zolotukhin and A. I. Al'Mukhamedov, in *Continental Flood Basalts*, J. D. Macdougall, Ed. (Kluwer, Dordrecht, Netherlands, 1988), pp. 273–310.
12. P. C. Lightfoot, A. J. Naldrett, N. S. Gorbachev, W. Doherty, V. A. Fedorenko, *Contrib. Mineral. Petrol.* **104**, 631 (1990).
13. M. Sharma, A. R. Basu, G. V. Nesterenko, *Geochim. Cosmochim. Acta* **55**, 1183 (1991).
14. V. V. Zolotukhin, A. M. Vilensky, O. A. Djuzhikov, *Nauka Novosibirsk* **612**, 245 (1986); Y. A. Zorin and B. M. Vladimirov, *Earth Planet. Sci. Lett.* **93**, 109 (1989).
15. G. I. Sadovnikov, *Izvestiya Academ. Nauka USSR* **9**, 49 (1981).
16. D. J. DePaolo and G. J. Wasserburg, *Proc. Natl. Acad. Sci. U.S.A.* **76**, 3056 (1979).
17. W. T. Holser and M. Margaritz, *Mod. Geol.* **11**, 155 (1987).
18. Samples of plagioclase were multigrain separates

weighing 5 to 20 mg from the 60- to 100-mesh fraction. Whole-rock samples were of matrix (phenocrysts removed) material crushed to 20- to 40-mesh size. The first analysis of each sample (46-WR.A and 2-WR.A) was on single grains of this material, the second was each on four grains. All samples (plagioclase and whole rock) were rinsed in dilute HCl and HF.

19. The effects of ^{39}Ar recoil loss and redistribution on apparent age spectra are discussed by G. Turner and P. H. Cadogan, *Geochim. Cosmochim. Acta Suppl. 5* **2**, 1601 (1974); J. C. Huneke, *Earth Planet. Sci. Lett.* **28**, 407 (1976); G. A. Schaeffer and O. A. Schaeffer, *Proc. Lunar. Sci. Conf.* **8**, 2253 (1977).
20. G. T. Cebula *et al.*, *TERRA Cognita* **6**, 139 (1986). The age of 27.84 Ma for Fish Canyon sanidine is consistent with an age of 520.4 Ma given by S. D. Samson and E. C. Alexander [*Chem. Geol. Isot. Geosci. Sect.* **66**, 27 (1987)] for the interlaboratory standard Mmhb-1. The corresponding J-value calculated from individual laser fusion of seven grains is $1.9104 \times 10^{-2} \pm 1.6978 \times 10^{-5}$.
21. Samples were incrementally heated by stepwise increasing power output from an Ar-ion laser with defocused beam. Laser power output, pneumatically actuated valve operation, and mass spectrometer operation (magnetic field jumping and detector output reading) were automated using procedures described by A. L. Deino and R. Potts [*J. Geophys. Res.* **95**, 8453 (1990)], A. Deino, L. Tauxe, M. Monaghan, and R. Drake [*J. Geol.* **98**, 567 (1990)], P. R. Renne, T. A. Becker, and S. M. Swapp [*Geology* **18**, 563 (1990)], P. R. Renne, M. M. Fulford, and C. J. Busby-Spera [*Geophys. Res. Lett.* **18**, 459 (1991)], and C. C. Swisher and D. R. Prothero [*Science* **249**, 760 (1990)]. A cryocooled cold-trap on the extraction line was operated at −50°C to help remove condensable gases. Uncertainties in dates are reported at the 2σ level and include contributions from uncertainties in isotope ratio regressions, corrections for mass discrimination, atmospheric contamination and interfering nucleogenic isotopes, and uncertainty in the $^{40}Ar^*/^{39}Ar_K$ of the standards, but do not include uncertainty in the age of the standard. Mass discrimination (1.0069 ± 0.0020 per atomic mass unit) was monitered by automated analysis of 20 air pipette samples interspersed with the sample analyses.
22. We define a plateau as comprising three or more contiguous steps with apparent ages that overlap the mean at the 2σ level excluding error contribution from the J-value. This definition is similar to that employed by R. J. Fleck *et al.* [*Geochim. Cosmochim. Acta* **41**, 15 (1977)] except that we do not stipulate that a plateau must contain any specific minimum proportion of the total Ar released. Our plateau dates are calculated as the weighted (by inverse variances) mean of all steps defining a plateau. Because errors in individual step dates are largely an inverse function of the Ar volume analyzed, the inverse variance weighting scheme produces results similar to schemes based on relative ^{39}Ar abundance.
23. Regression of $^{36}Ar/^{40}Ar$ versus $^{39}Ar/^{40Ar}$ followed the technique of D. York [*Earth Planet. Sci. Lett.* **5**, 320 (1969)] and yielded the following results: For 46-WR, date = 248.2 ± 1.2 Ma, $(^{40}Ar/^{36}Ar)_0$ = 287.6 ± 31.0, N = 15, MSWD = 0.475; for 46-PL, date = 249.5 ± 1.2 Ma, $(^{40}Ar/^{36}Ar)_0$ = 259.5 ± 26.3, N = 9, MSWD = 0.722; for 42-PL, date = 246.4 ± 2.2 Ma, $(^{40}Ar/^{36}Ar)_0$ = 292.0 ± 23.4, N = 10, MSWD = 1.052; for 2-WR, date = 246.3 ± 4.3 Ma, $(^{40}Ar/^{36}Ar)_0$ = 315.0 ± 41.2, N = 8, MSWD = 1.860.
24. The volume estimate is based on the proportion of maximum composite stratigraphic thickness represented by flows older than the Kharaelakhsky suite (Fig. 2), and the assumption that there is a consistent relation between thickness and volume.
25. R. A. Duncan and M. A. Richards, *Rev. Geophys.* **29**, 31 (1991).
26. G. F. Marenko, *Int. Geol. Rev.* **19**, 1089 (1976).
27. The dates are based on an age of 27.84 Ma for Fish Canyon sanidine (*20*). Recent studies by M. A. Lanphere *et al.* [*Proceedings of the Seventh International Conference on Geochronology, Cosmochronology, and Isotope Geology* (Abst.), Canberra (1990), p. 57] and C. C. Swisher (*ibid.*, p. 98) indicate that this age may be in error by as much as 1%. Recalculating uncertainty in the neutron fluence parameter J with a 1% uncertainty in age (at the 95% confidence level) yields a value of $2\sigma_J = 1.9326 \times 10^{-4}$. With the pooled mean plateau value of $^{40}Ar^*/^{39}Ar_K$ = 7.7256 ± 0.0099 for sample 46, a date of 248.4 ± 2.4 Ma (2σ) is obtained that reflects uncertainty in the age of the standard and is appropriate for external comparison.
28. R. L. Armstrong, in *Contributions to the Geologic Time Scale*, G. V. Cohee, M. F. Glaessner, H. D. Hedberg, Eds. (*Stud. Geol. 6*, American Association of Petroleum Geologists, Tulsa, 1978), pp. 73–91; K. N. Hellman and H. J. Lippolt, *J. Geophys.* **50**, 73 (1981); J. A. Webb, *J. Geol. Soc. Austral.* **28**, 107 (1981); G. S. Odin and W. J. Kennedy, *C. R. Seances Acad. Sci. Paris* **294**, 453 (1982); W. B. Harland *et al.*, *A Geologic Time Scale* (Cambridge Univ. Press, Cambridge, 1982); A. R. Palmer, *Geology* **11**, 503 (1983); S. C. Forster and G. Warrington, in *The Chronology of the Geological Record*, N. J. Snelling, Ed. (Blackwell, Palo Alto, 1985), pp. 99–113; G. S. Odin, in *ibid*, pp. 114–117.
29. N. D. Newell, in *The Permian and Triassic Systems and Their Mutual Boundary*, A. Logan and L. V. Hills, Eds. (*Mem. 2*, Canadian Society of Petroleum Geologists, Calgary, 1973), pp. 1–10.
30. This research was supported by the Institute of Human Origins and National Science Foundation grant EAR 8805781. We are indebted to G. V. Nesterenko for providing samples and geologic context; T. A. Becker for assistance in the Ar laboratory; D. Beckner for graphics; W. Alvarez, G. H. Curtis, G. Czamanske, D. J. DePaolo, R. A. Duncan, and M. Sharma for discussions; M. A. Richards, C. C. Swisher, and R. C. Walter, plus three anonymous reviewers, for constructive criticism of the manuscript.

11 March 1991; accepted 15 May 1991

Solution Structures of β Peptide and Its Constituent Fragments: Relation to Amyloid Deposition

COLIN J. BARROW* AND MICHAEL G. ZAGORSKI†

The secondary structures in solution of the synthetic, naturally occurring, amyloid β peptides, residues 1 to 42 [β(1-42)] and β(1-39), and related fragments, β(1-28) and β(29-42), have been studied by circular dichroism and two-dimensional nuclear magnetic resonance spectroscopy. In patients with Alzheimer's disease, extracellular amyloid plaque core is primarily composed of β(1-42), whereas cerebrovascular amyloid contains the more soluble β(1-39). In aqueous trifluoroethanol solution, the β(1-28), β(1-39), and β(1-42) peptides adopt monomeric α-helical structures at both low and high pH, whereas at intermediate pH (4 to 7) an oligomeric β structure (the probable structure in plaques) predominates. Thus, β peptide is not by itself an insoluble protein (as originally thought), and localized or normal age-related alterations of pH may be necessary for the self-assembly and deposition of β peptide. The hydrophobic carboxyl-terminal segment, β(29-42), exists exclusively as an oligomeric β sheet in solution, regardless of differences in solvent, pH, or temperature, suggesting that this segment directs the folding of the complete β(1-42) peptide to produce the β-pleated sheet found in amyloid plaques.

ALZHEIMER'S DISEASE (AD) IS characterized by extracellular deposits in the form of amyloid plaques (*1*). The major protein constituent of plaques is β peptide (Fig. 1), which is a small (39 to 43 amino acids) polypeptide (*2, 3*) derived from a larger (695, 714, 751, or 770 amino acids) amyloid precursor protein (APP) (*4*). The majority of recent research into AD has focused on APP; that is, investigations have focused on the relations of different APP forms to AD (*5*) and the normal and alternative pathways by which APP molecules can be proteolytically processed (*6*). However, less information is known about the amyloid β peptide than about APP, especially on a molecular level (*7, 8*), because β peptide is extremely insoluble and has a high propensity to aggregate. This latter property is presumably related to its tendency to produce oligomeric β structures, the probable conformation in plaques (*9, 10*).

The circular dichroism (CD) spectra for freshly prepared solutions of β peptide and some fragments, in aqueous 5 mM phosphate buffer at pH 7.3 and 22.0°C, are shown in Fig. 2A. Analysis of these spectra by the method of Greenfield and Fasman (*11*), together with computer fitting (*12*) to polylysine standard curves, gives approximately 90 and 100% β-sheet structure for the β(1-42) and β(29-42) peptides, respectively. In contrast, the β(1-28) peptide is essentially random coil, and the β(1-39) peptide is a mixture of random coil and β-sheet structures in an approximate ratio of

Suntory Institute for Bioorganic Research, Wakayamadai, Shimamoto-cho, Mishima-gun, Osaka 618, Japan.

†To whom correspondence should be addressed.
*Present address: Sterling Drug, 9 Great Valley Parkway, Malvern, PA 19355.